Mössbauer Spectroscopic Studies of Magnesium Nickel Ferrites

K. SESHAN, A. S. BOMMANNAVAR* AND D. K. CHAKRABARTY†

Solid State Laboratory, Department of Chemistry, Indian Institute of Technology, Powai, Bombay 400 076, India

Mössbauer spectra of magnesium nickel ferrites having spinel structure with varying percentages of nickel were obtained at room temperature. The split extreme high-resonance line could be resolved into two Lorentzians from which the cation distribution was calculated. The calculated cation distributions match very well with those obtained from magnetization measurements as well as from ferromagnetic resonance studies on the same samples. The observed quadrupole split and the hyperfine field values can be rationalized based on the obtained cation distributions.

Introduction

One of the most fruitful applications of Mössbauer spectroscopy lies in the study of magnetic materials such as ferrites. It allows a closer look into the effects, on individual cations, of the changes in the species at the neighboring sites. Besides, many of the spinel ferrite phases are magnetically ordered where the major interactions are the Fe–Fe and Fe–M superexchange, where M is another magnetic cation. Mössbauer effect can give here precise information on the local magnetic behavior of the ions.

Sawatzky et al. (1) and Knoch and Dannheim (2) have determined the cation distribution in some spinel ferrites by resolving the extreme high-resonance line in the hyperfine Mössbauer spectra as a sum of two Lorentzians corresponding to the octahedral (B) and tetrahedral sites (A). The areas under the two Lorentzians are a measure of the occupation numbers of iron

* Department of Physics, West Virginia University, WV 26506.
† To whom correspondence should be addressed.

ions in the two respective sites. They found excellent agreement between the cation distributions obtained from Mössbauer data and magnetization measurements at 4.2K. DeGrave et al. (3), on the other hand, consider that the description of cation distribution with only two Lorentzians in an incompletely split spectrum, and that, too, from measurements at room temperature, is a gross approximation. These authors suggest that the B-site spectrum is not a single Lorentzian, but comprises more than one subspectra corresponding to B-site Fe^{3+} ions having four, five, or six Fe^{3+} A-site nearest neighbors. They showed that the experimentally observed B-site hyperfine field, $(H_{eff})_B$, is close to the case calculated for six Fe^{3+} A-site nearest neighbors. In the cases with four or five Fe^{3+} A-site nearest neighbors, the calculated B-site H_{eff} values are either nearly equal to or smaller than the A-site field. Hence in analyzing the zero-field spectrum as a sum of two six-line patterns, these two subspectra are seen as belonging to A-site ferric ions resulting in a lower value of area I_B/I_A. They cross-

checked the cation distribution in their samples by X-ray diffraction.

We have undertaken a systematic study of the ferrite system $Ni_xMg_{1-x}Fe_2O_4$ in order to determine the effect of heat treatment and addition of Ni^{2+} ions on the distribution of Mg^{2+} and Fe^{3+} ions on the A and B sites. In doing so, we have determined the cation distribution in these compounds independently from magnetization measurements (4) and from ferromagnetic resonance studies (5). The study of Mössbauer spectra of these compounds with already established cation distribution will permit one to ascertain which of the two prevalent views on the assignment of the hyperfine field is correct. The results of our studies are reported here and are compared with our earlier results of magnetization and ferromagnetic resonance studies on the same samples (4, 5).

Experimental

The compounds $Ni_xMg_{1-x}Fe_2O_4$ ($0 \leq x \leq 1$) have all been prepared from the oxides by standard ceramic techniques. For studying the effect of heat treatment, one set of compositions was quenched from 1575K and another furnace cooled at the rate of 60K/hr. They are all monophasic cubic spinels. The details are given elsewhere (5).

The Mössbauer spectra were recorded at 300K in the transmission mode using a constant acceleration drive and a multichannel analyzer. The spectrometer was calibrated for velocities by using standards such as SS310, pure iron foil (Amersham England), and sodium nitroprusside.

The spectra were fitted by a program which performs a least mean square fit of Lorentzians to the experimental data using the variable matrix minimization. The variables for which minimization is performed are

(i) an assumed linear (zero slope) off resonance count level,

(ii) peak intensity,

(iii) full-width at half-maximum intensity (FWHM), and

(iv) peak position.

The number of lines assumed to be present is not variable. In all instances the hyperfine parameters were obtained from an analysis in which the extreme negative line is fitted. In no case have we used an analysis for which χ^2 ($\chi^2 = \Sigma_i(y_i - f(x)^2/y_i)$) exceeds 1.1. Care has been taken that the maximum acceptable value of χ^2 is never larger than that of the calibration spectrum at the corresponding count level.

Results and Discussion

The Mössbauer spectra of the compounds are given in Fig. 1 for furnace-cooled samples and in Fig. 2 for quenched samples. On the right-hand side of each spectrum, the best, two-Lorentzian fit for the extreme line is given in an expanded velocity scale. The parameters calculated from the best-fit spectra are given in Table I.

Isomer Shifts (IS)

The IS values for Fe in A and B sites for both quenched and furnace-cooled samples are in the range of 0.3–0.8 mm/sec with respect to iron. This indicates the presence of iron in the 3+ state only. The Seebeck coefficient measurements on these samples (5) have also revealed the absence of any appreciable amount of Fe^{2+} ions. Further, variation of IS with composition, if any, is insignificant.

Determination of Cation Distributions

The following points were taken into account for calculating the cation distribution.

The extreme negative lines, which are clearly split, in the Mössbauer spectra, were fitted as a sum of two Lorentzians. This is in accordance with the method adopted by different workers (1, 2, 6). The
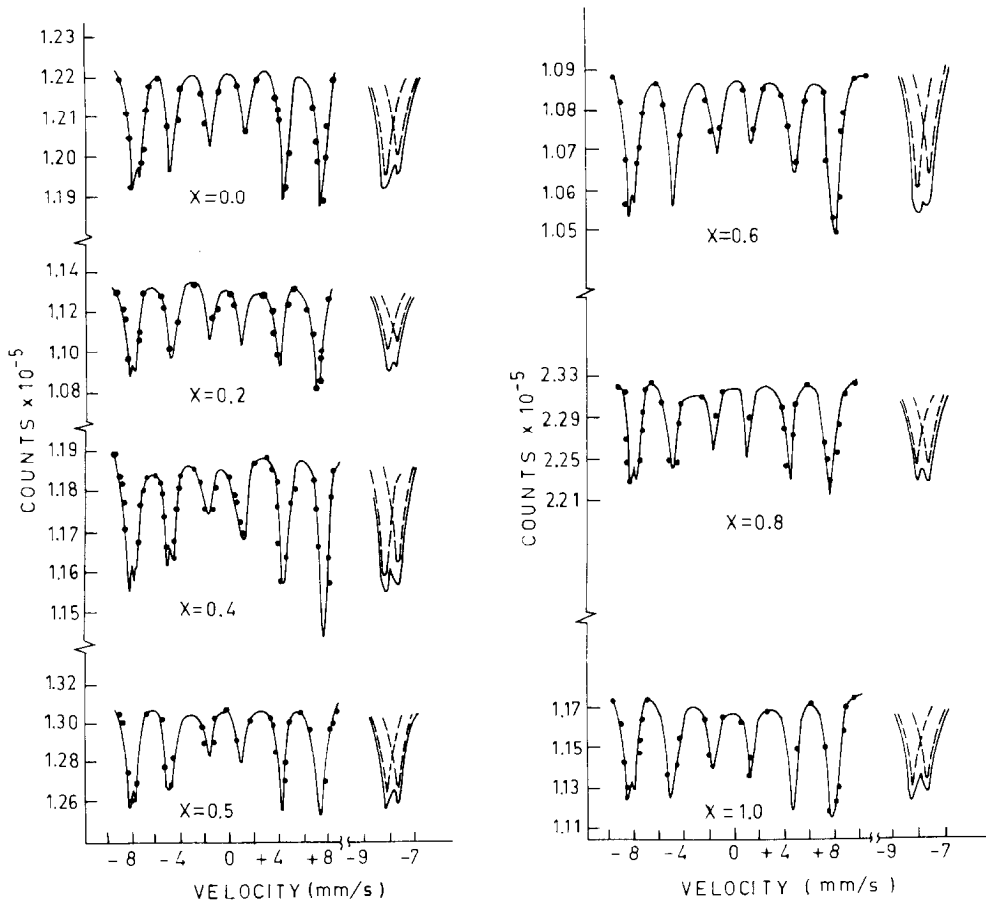
FIG. 1. Mössbauer spectra of the system $Ni_xMg_{1-x}Fe_2O_4$ (furnace cooled).

TABLE I

MÖSSBAUER SPECTRAL PARAMETERS OF THE SYSTEM $Ni_xMg_{1-x}Fe_2O_4$

	Furnace-cooled samples						Quenched samples					
	IS^a (mm/sec)		QS (mm/sec)		H_{eff} (kOe)		IS^a (mm/sec)		QS (mm/sec)		H_{eff} (kOe)	
Composition (x)	A	B	A	B	A	B	A	B	A	B	A	B
0.0	0.67	0.39	0.31	−0.18	456	468	0.67	0.47	0.23	0.03	431	443
0.2	0.56	0.43	0.13	−0.20	458	471	0.45	0.45	−0.10	0.02	455	455
0.4	0.71	0.46	0.32	−0.17	463	479	0.59	0.59	0.08	0.08	461	461
0.5	0.65	0.43	0.22	−0.16	467	481	0.50	0.30	0.03	−0.17	456	468
0.6	0.47	0.32	0.10	−0.27	474	493	0.55	0.47	0.02	−0.06	471	476
0.8	0.67	0.45	0.16	−0.06	481	496	0.71	0.59	0.12	0.08	481	493
1.0	0.71	0.30	0.28	−0.36	493	505	0.60	0.31	0.26	−0.34	495	503

^{a} IS with respect to iron. A = Tetrahedral site, B = octahedral site.
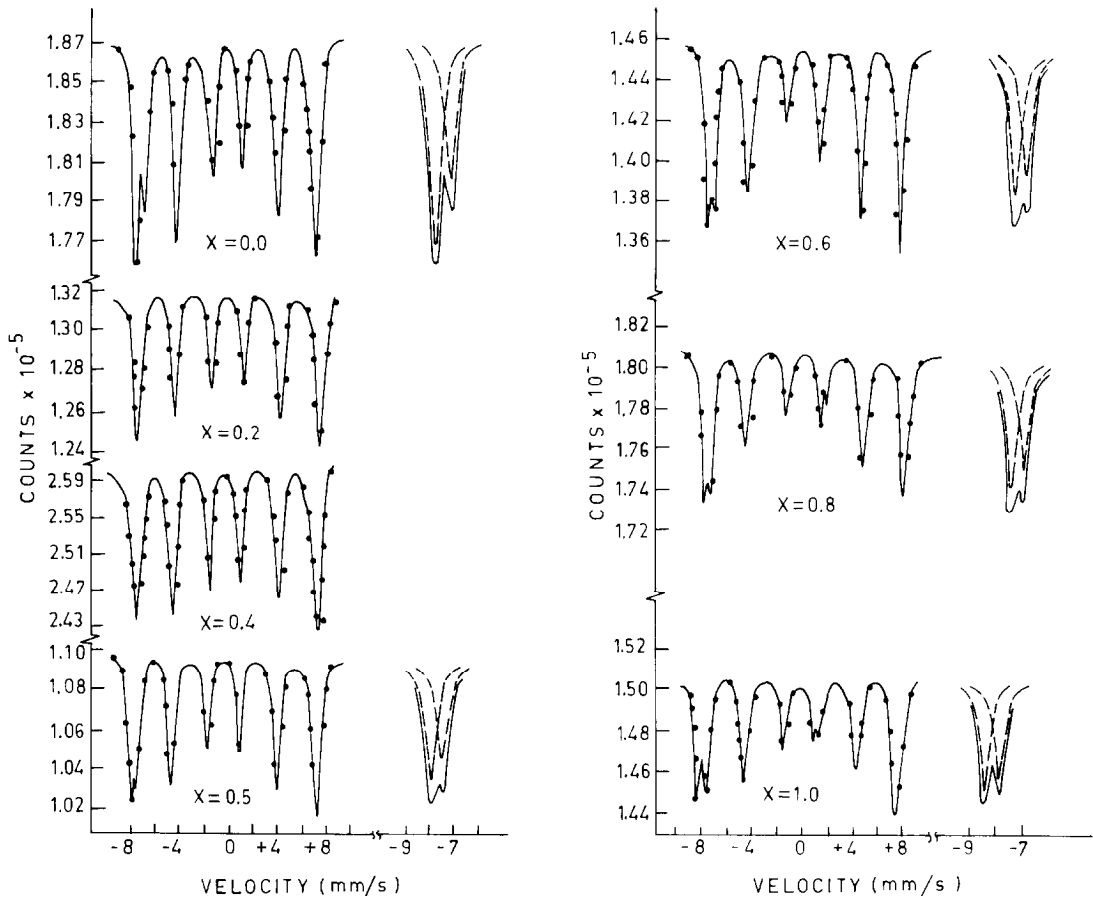
FIG. 2. Mössbauer spectra of the system $Ni_xMg_{1-x}Fe_2O_4$ (quenched).

TABLE II

CATION DISTRIBUTION PARAMETER δ ($Fe^{3+}_{B\,site}/Fe^{3+}_{A\,site}$) IN THE SYSTEM $Ni_xMg_{1-x}Fe_2O_4$

| Composition (x)	Furnace-cooled samples δ			Quenched samples δ		
	Mössbauer data	FMR data	Magnetization at OK data	Mössbauer data	FMR data	Magnetization at OK data
0.0	1.260	1.286	1.273	1.581	1.692	1.684
0.2	1.180	1.160	1.155	—	1.469	1.469
0.4	1.100	1.099	1.099	—	1.384	1.378
0.5	1.080	1.075	1.070	1.260	1.251	1.257
0.6	1.140	1.077	1.072	1.216	1.228	1.222
0.8	1.030	1.077	1.072	1.120	1.128	1.128
1.0	1.010	1.000	1.000	1.010	1.000	1.000

integrated areas under the Lorentzians corresponding to A and B sites are taken as proportional to the amount of Fe^{3+} ions on these sites. The implicit assumption in such calculations are:

(i) The "f" factors for A and B sites are nearly the same. Further, it has been shown (6) that the ratio of recoilless fractions (f_B/f_A) is 0.94 ± 0.02 at 300K, giving rise to an error of less than 6% in the ratio of the occupation numbers of B and A sites.

(ii) The integrated area ratio for the single line is equal to the ratio of cumulative areas for the entire spectrum, i.e., all the six lines.

The assignment of peaks for the A and B sites were achieved by comparing the spectra and hyperfine fields with those reported (1) for the pure compounds $MgFe_2O_4$ (quenched and furnace-cooled) and Ni Fe_2O_4.

The presence of Fe^{2+} ions has been excluded by IS values as well as by other measurements such as Seebeck coefficients (5), saturation magnetization at 0K (5), and FMR parameters (4). Since, in this case, all Ni^{2+} goes to the octahedral site due to its stronger B-site preference (7), the cation distribution can be calculated by knowing the ratio of Fe^{3+} on the two sites, as

$$Mg_y^{2+}Fe_{1-y}^{3+}[Ni_x^{2+}Fe_{1+y}^{3+}Mg_{1-x-y}^{2+}]O_4^{2-}.$$
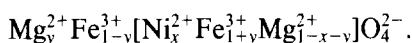
The ratios of Fe_B^{3+}/Fe_B^{3+} obtained from Mössbauer spectra as well as other measurements, for comparison, are given in Table II. The agreement is good and within the scope of the arguments presented above. Thus the results of our study show that the cation distribution obtained by resolving a single Lorentzian of the hyperfine Mössbauer spectrum is quite reliable, at least for magnesium nickel ferrite system. Two of the compositions $Ni_{0.2}Mg_{0.8}Fe_2O_4$ and $Ni_{0.4}Mg_{0.6}Fe_2O_4$ among the quenched samples showed nonsplit spectra and could therefore not be resolved. Resolving this would require the spectra to be recorded in

an externally applied magnetic field at a lower temperature.

Quadrupole Splits (QS)

Any asymmetry at the A- and/or B-site environment of Fe^{3+} ions gives rise to non-zero quadrupole splits. QS in compounds containing Fe^{3+} at A site is attributed to the asymmetric charge distribution associated with the random distribution of divalent and trivalent ions on the neighboring 12 B sites which surround the A site (8). In the present case the distribution of Ni^{2+} and Fe^{3+} ions on the B sites creates an asymmetry at the A site and gives rise to a QS. The observed QS at the B site is attributed to the trigonal field created by the distortion due to the oxygen parameter (u) present in such compounds.

Further, the QS values are lower for quenched samples than for the furnace-cooled ones. This is caused by the higher concentration of Mg^{2+} ions on the A sites in quenched samples which displace an equal number of Fe^{3+} to B sites making the B-site charge distribution less asymmetric as most of the 12 B-site neighbors surrounding A site are Fe^{3+} ions.

Hyperfine Field (H_{eff})

It may be noticed from the Table I that there is a regular increase in the H_{eff} values with the addition of Ni^{2+} ions and that the H_{eff_B} values are higher than H_{eff_A} values. An explanation may be found in the following lines.

One major factor which contributes to the H_{eff_B} is the greater covalency of the Fe^{3+} ions at the A site. Further, Geller et al. (9) have shown that the $Fe^{3+}-O^2-Fe^{3+}$ superexchange interaction is stronger than the $Fe^{3+}-O^{2-}-Ni^{2+}$ interaction. The average magnetization per Fe^{3+} ion on the A site is therefore smaller than that for an Fe^{3+} ion on the B site. This is so because each A-site

Fe^{3+} ion will have intersublattice magnetic bonds with Fe^{3+} and Ni^{2+} ions, while every B-site Fe^{3+} will have all its intersublattice magnetic bonds with Fe^{3+} ions only. The smaller average magnetization of the A site gives rise to smaller H_{eff_A} when compared to H_{eff_B}.

The effect of composition on the H_{eff} can be understood by looking at the cation distribution of the samples. In all cases there is an increase in sublattice magnetization with composition because with increasing x, Fe^{3+} concentration on the A sites and Ni^{2+} concentration on B sites increase. This may be an additional indication that Ni^{2+} ions also contribute for the hyperfine fields through A–B and B–B exchange interactions.

References

1. G. A. SAWATZKY, F. VAN DER WOUDE, AND A. H. MORRISH, *Phys. Rev.* **187**(2), 747 (1969).
2. H. KNOCH AND H. DANNHEIM, *Phys. Status Solidi A* **37**, K135 (1976).
3. E. DEGRAVE, A. GOVAERT, D. CHAMBAERE, AND G. ROBBRECHT, *Physica B* **96**, 103 (1979).
4. K. SESHAN, M. J. PATNI, AND D. K. CHAKRABARTY, *J. Solid State Chem.* **42**, 206 (1982).
5. K. SESHAN, A. L. SHASHIMOHAN, D. K. CHAKRABARTY, AND A. B. BISWAS, *Phys. Status Solidi A* **68**, 97 (1981).
6. G. A. SAWATZKY, F. VAN DER WOUDE, AND A. H. MORRISH, *J. Appl. Phys.* **39**(2), 1204 (1968).
7. A. MILLER, *J. Appl. Phys.* **30**(4), 245 (1959).
8. H. B. MATHUR, A. P. B. SINHA, AND C. M. YAGNIK, *Indian J. Pure Appl. Phys.* **5**, 155 (1967).
9. S. GELLER, A. J. WILLIAMS, R. C. SHERWOOD, AND G. P. ESPINOVA, *J. Phys. Chem. Solids* **23**, 1525 (1962).